0026-895X/99/010159-09$3.00/0

MOLECULAR PHARMACOLOGY, **55:**159–167 (1999).

Aminotriarylmethane Dyes Are High-Affinity Noncompetitive Antagonists of the Nicotinic Acetylcholine Receptor

MONICA M. LURTZ[1] and STEEN E. PEDERSEN

Department of Molecular Physiology and Biophysics, Baylor College of Medicine, Houston, Texas

Received July 6, 1998; accepted September 22, 1998

This paper is available online at http://www.molpharm.org

ABSTRACT

A series of aminotriarylmethane dyes were examined for binding to the nicotinic acetylcholine receptor (AChR) from *Torpedo californica.* Several compounds were found to bind to the noncompetitive antagonist site of the AChR as demonstrated by inhibition of [^{3}H]phencyclidine binding; apparent K_D values ranged from 50 nM to >100 μM. One dye with high affinity, crystal violet, revealed a greater than 200-fold fluorescence enhancement upon binding the AChR. Using fluorescence to measure binding, we determined that one crystal violet bound per receptor with a dissociation constant of 100 nM; in the presence of the agonist carbamylcholine this value decreased to 10 nM. The K_D for [^{3}H]acetylcholine binding likewise was decreased in the presence of crystal violet. These results are consistent with preferential binding of crystal violet to the desensitized conformation of the AChR. Crystal violet binding blocked agonist-induced ^{22}Na ion efflux from AChR-rich vesicles. It is concluded that crystal violet and other dyes of similar structure bind to the high-affinity noncompetitive antagonist site of the AChR associated with the channel lumen. Because of their optical properties, crystal violet and several of the other homologous dyes are likely to be useful ligands for further characterization of the AChR channel. Structure-activity comparison of the various dyes suggests the importance of nonquaternary nitrogens in binding the pore. Additional steric bulk on amines or at meta positions increase or have neutral effect on affinity, suggesting that steric considerations alone do not limit high affinity for the binding site.

The nicotinic acetylcholine receptor (AChR) from *Torpedo californica* electric organ is a pentameric, ligand-gated, nonspecific cation channel composed of four distinct, homologous subunits with a stoichiometry of $\alpha_2\beta\gamma\delta$ (Raftery et al., 1980; Noda et al., 1983; Unwin, 1993). Each subunit possesses four putative transmembrane segments termed M1, M2, M3, and M4. Studies of chimeric AChRs (Imoto et al., 1986, 1988) have produced substantial evidence that the M2 domain lines the pore of the channel. Affinity-labeling experiments further identified this sequence as the site of high-affinity noncompetitive antagonist binding. Meproadifen mustard labeling was localized to αGlu-262 in M2 (Pedersen et al., 1992); chlorpromazine and triphenylmethylphosphonium specifically label homologous residues within the M2 sequences of each subunit (Giraudat et al., 1986, 1987, 1989; Hucho et al., 1986). Labeling studies with TID, an uncharged noncompetitive antagonist, identified reactive sites within M2 for AChR stabilized in either the resting conformation or the desensitized state (White et al., 1991; White and Cohen, 1992). Mutagenesis of residues within the M2 sequence affects the affinity of open channel block by the high affinity noncompetitive antagonist (NCA) QX-222 (Leonard et al., 1988; Charnet et al., 1990). These data support a model for channel-blocking activity that is consistent with simple steric occlusion of the pore by NCAs (Neher and Steinbach, 1978).

The M2 locus is likely the high-affinity binding site for other noncompetitive antagonists such as phencyclidine (PCP), ethidium, and proadifen, whose binding loci have not yet been identified at the resolution of individual amino acids (Krodel et al., 1979; Heidmann et al., 1983; Herz et al., 1987). With some exceptions, noncompetitive antagonists are generally cationic and hydrophobic, but otherwise constitute a structurally heterogeneous class of ligands. The binding characteristics of several high-affinity NCAs have been studied extensively, resulting in a better understanding of receptor structure. NCAs such as tetracaine and TID preferentially bind the resting state of the AChR; histrionicotoxin shows a slight conformational preference, whereas most other NCAs, including phencyclidine, ethidium, meproad-

Public Health Service Grants NS28879 and NS35212 supported this research. S.E.P. was supported by Research Career Development Award NS01618. M.M.L. was supported by Training Grant HL07676.

[1] Current address: Department of Veterinary Pathobiology, University of Minnesota Medical School, St. Paul, MN 55455.

ABBREVIATIONS: ACh, acetylcholine; AChR, nicotinic AChR receptor; PTMA, phenyltrimethylammonium; CHAPS, 3-[(3-cholamidopropyl)-dimethylammonio]-1-propane-sulfonate; CrV, crystal violet; Dpmsm, *N*-(4-(((4-dimethylamino)phenyl)(4-methoxy-3-sulfophenyl)methylene)-2,5-cyclohexadien-1-ylidene)-*N*-methylmethanaminium, inner salt; HPLC, high performance liquid chromatography; HTPS, HEPES-*Torpedo* physiological saline; NCA, high-affinity noncompetitive antagonist of AChR; PCP, phencyclidine; TFA, trifluoroacetic acid.

ifen, chlorpromazine, triphenylmethylphosphonium, and quinacrine, preferentially bind the desensitized conformation of AChR at equilibrium (Krodel et al., 1979; Heidmann et al., 1983; White et al., 1991; Wu et al., 1994; Lurtz et al., 1997).

Fluorescent NCAs such as ethidium and quinacrine have been used to examine the structure and environment of the AChR. These compounds increase their quantum yield upon binding the NCA site. Fluorescence measurements have shown that ethidium becomes immobilized and shielded from solvent upon binding the AChR (Herz et al., 1987; Herz and Atherton, 1992). Quenching and fluorescence energy transfer measurements are potentially useful tools for further characterization of the properties of the NCA site. The utility of these two fluorophores is somewhat limited by their affinity, the sensitivity of their affinities to ionic strength changes (Lurtz et al., 1997), and nonspecific interaction with the lipid bilayer. We desired to carry out diffusion-enhanced energy transfer experiments (Stryer et al., 1982) using NCA site ligands as the energy transfer acceptors. The sensitivity of such experiments is strongly dependent on the extinction coefficient of the ligand. We therefore investigated the ability of strongly absorbing dyes to act as NCAs of the AChR.

We present data that the aminotriarylmethane dyes, compounds with structures similar to the NCA, triphenylmethylphosphonium, are a novel family of NCAs. Several members of this family bind with K_D values in the low nanomolar range, particularly crystal violet (CrV). Further analysis of CrV demonstrated that crystal violet binds the noncompetitive antagonist site in the pore of the AChR with high affinity and a substantial, concomitant fluorescence enhancement. Its high affinity and fluorescence properties further makes CrV, in particular, a good probe for future fluorescence quenching and fluorescence energy transfer experiments. The high affinity of this compound and the existence of many structurally related basic dyes will provide an approach to a more detailed structure-activity relationship of the NCA site. Here we present an analysis of the binding relationships of these ligands.

Experimental Procedures

Materials. Crystal violet hydrochloride, methyl violet 2B, brilliant green, malachite green carbinol hydrochloride, ethyl violet hydrochloride, methyl green zinc chloride, rosaniline, pararosaniline chloride, new fuchsin, patent blue VF, Victoria pure blue BO, leuco crystal violet, and crystal violet lactone were obtained from Aldrich Chemical Co. (Milwaukee, WI). *N*-(4-(((4-dimethylamino)phenyl)(4-methoxy-3-sulfophenyl)methylene)-2,5-cyclohexadien-1-ylidene)-*N*-methylmethanaminium inner salt (Dpmsm) was obtained from Eastman Chemical Co. (Rochester, NY). Before use, crystal violet was crystallized from chloroform, then recrystallized from water. Purity was assessed by reversed-phase high performance liquid chromatography (HPLC) as described below.

Carbamylcholine hydrochloride, PCP, sodium dodecyl sulfate, and 3-[(3-cholamidopropyl)-dimethylammonio]-1-propane-sulfonate (CHAPS) were from Sigma Chemical Co. (St. Louis, MO). [^{3}H]PCP (43 Ci/mmol), low specific activity [^{3}H]ACh (73 mCi/mmol), and ^{22}NaCl (19 Ci/mmol) were purchased from New England Nuclear (Boston, MA). High specific activity [^{3}H]ACh (90 Ci/mmol) was obtained from American Radiochemicals. HPLC-grade acetonitrile and trifluoroacetic acid (TFA) were from Baker (Phillipsburg, NJ) and Pierce (Rockford, IL), respectively.

AChR-rich membranes were prepared from frozen *Torpedo californica* electric organ (Marinus, Long Beach, CA) by differential sucrose ultracentrifugation as described previously (Sobel et al., 1977; Pedersen et al., 1986). Membranes used for most experiments ranged in specific activity from 1.0 to 1.8 nmol ACh binding sites per mg of protein, as determined by [^{3}H]ACh binding; values listed in the remainder of the article are for AChR concentrations, which equal one-half the ACh binding-site concentration. Experiments were conducted in either 20 mM HEPES, pH 7.0, or in HTPS (250 mM NaCl, 5 mM KCl, 3 mM $CaCl_2$, 2 mM $MgCl_2$, and 20 mM HEPES, pH 7.0).

Spectroscopy. Fluorescence measurements were taken on either an SLM 8000C fluorometer (Rochester, NY) with a 350W xenon arc lamp or on an ISS PC1 fluorometer (Urbana, IL) equipped with a 300W lamp using 10 × 10 mm cuvettes. For single-point measurements or time-dependent measurements of CrV fluorescence, the excitation wavelength was 600 nm with a 550-nm cut-on filter (Oriel no. 59502; Stratford, CT); emission was monitored at 645 nm with an RG630 cut-on filter (ESCO no. 5274630); all bandwidths were 16 nm. Fluorescence excitation spectra were collected as a ratio of fluorescence signal intensity to a reference signal to correct for lamp intensity at the various wavelengths. Emission spectra were collected on the ISS instrument; they were corrected for instrument response using calibration factors provided by the manufacturer. Excitation and emission spectra were also corrected for inner filter effects using the following equation (Lakowicz, 1983): $F_{corr} = F_{obs} \cdot 10^{(Aex+Aem)/2}$, where F_{obs} is the observed fluorescence intensity, A_{ex} and A_{em} are the absorbances of the fluorophore at the excitation and emission wavelengths, and F_{corr} is the fluorescence intensity corrected for inner filter effects. This correction was only significant for spectra taken at high CrV concentrations.

The absorbance spectra of crystal violet were taken on a Cary 1/3 UV/VIS spectrophotometer (Varian, Sugarland, TX) in the dual-beam mode, where samples without crystal violet served as the reference.

Binding Assays. [^{3}H]PCP inhibition assays were conducted by centrifugation assay essentially as described (Lurtz et al., 1997), except that some experiments were incubated for 2 h at ambient temperature. Data were fit to a model for inhibition at a single site: $B = B_{max}/(1 + I/K_{app}) + Bcg$ (eq. 1), where B_{max} represents the maximal binding, I is the inhibitor concentration, K_{app} is the inhibition constant, and Bcg is the background (nonspecific) binding, as defined by the presence of excess unlabeled competitor. [^{3}H]ACh-binding assays were conducted as described previously (Pedersen and Papineni, 1995); nonspecific binding was determined by inclusion of excess carbamylcholine.

Measurements of crystal violet binding to the AChR were carried out in microcentrifuge tubes with 20 nM AChR and in a final volume of 1.5 ml. Samples were incubated for 2 h at ambient temperature, the fluorescence intensity was measured in a cuvette, and the samples were then returned to the microcentrifuge tubes for centrifugation at 18,500*g* for 30 min at 20°C in a TOMY MTX-150 tabletop microcentrifuge. An aliquot of each supernatant was transferred to fresh microfuge tubes containing CHAPS to yield a 1% final CHAPS concentration. The fluorescence of each sample was measured and the corresponding CrV concentration was determined by comparison with a standard curve. Binding data were fitted to the binding equation by a nonlinear least-squares algorithm (SigmaPlot versions 2.0 or 4, Jandel, Inc.): $B = L/(L + K_D)$ (eq. 2), where B is the specific bound concentration, L is the free ligand concentration, and K_D is the dissociation constant.

Fluorescence inhibition assays were conducted in the presence of 10 or 20 nM AChR, excess carbamylcholine, and varying concentrations of PCP. The data were fitted to eq. 1, and then the K_{app} values for the competitor were replotted as a function of the mean free crystal violet concentration.

The stoichiometry of crystal violet binding was determined by titration of crystal violet into a concentrated suspension of AChR-rich vesicles in the presence or absence of 1 mM PCP (final volume: 2 ml, in HTPS). The fluorescence intensity of the sample was measured before the addition of crystal violet and for each point in the titration, with a 10- to 15-min waiting period between additions to

ensure that binding was at equilibrium. To minimize dilution effects, volume changes were kept at less than 2% of the total by adding concentrated CrV solutions. The CrV binding-site concentration was determined from the intercepts of the limiting slopes of the initial data points and of the final data points. The initial points in the titration reflect binding of nearly all the added CrV to the AChR. Therefore, the fluorescence intensity $F_i = Q_B \cdot L$, where L is the concentration of CrV added and Q_B is the quantum yield of CrV when bound to the AChR. At the final data points in the titration, the binding site is saturated and any further increase in fluorescence reflects increases in nonspecific binding. The equation for the fluorescence intensity is as follows: $F_f = Q_B \cdot R_0 + Q_N(L - R_0)$, where R_0 is the total concentration of CrV-binding sites and Q_N is the quantum yield of the fluorescence due to nonspecific interactions. At the intercept of these lines ($F_i = F_f$) $R_0 = L$, and the CrV binding-site concentration can be read directly from the CrV concentration axis.

^{22}Na Efflux Assay. ^{22}Na efflux assays were conducted using the procedure of Neubig and Cohen (1980) essentially as described by White et al. (1991); all manipulations were carried out at 4°C. Briefly, a concentrated suspension of AChR-rich vesicles was incubated with ^{22}Na overnight in HTPS. The excess ^{22}Na was removed by passing the vesicles over a 3-ml Dowex 50W-X8 column, and the vesicles were diluted immediately with HTPS. After a 20-min incubation to permit passive release of ^{22}Na to reach a slow, steady-state level, the assays were initiated by addition of 0.3 mM phenyltrimethylammonium and the suspension was filtered through Whatman GF/F filters 20 s later. The filters had been pretreated with 1% polyethyleneimine and washed with 10 ml HTPS before filtration. To measure block of efflux by NCAs, the vesicles were preincubated for 10 min with the NCA before initiating release. Maximal ^{22}Na efflux from *Torpedo californica* vesicles was determined by 10-min incubation with gramicidin D. Data were normalized to the release observed in the presence of gramicidin.

Determination of Partition Coefficients. AChR-rich membranes were incubated for 1 h at ambient temperature in the presence of 500 nM CrV and 0.1 mM carbamylcholine in the presence or absence of 1 mM PCP. Membranes were sedimented in a tabletop TOMY MTX-150 microcentrifuge at 18,500*g* for 30 min at 20°C, and supernatants then were transferred to microfuge tubes containing CH_3CN (50–55%) with 0.1% TFA and assayed by HPLC. Crystal violet was stable in 0.1% TFA for several days. To release bound CrV, the sedimented membranes were resuspended in 55% CH_3CN/0.1% TFA plus 1 mM PCP. The membranes were removed by centrifugation, as above, and the crystal violet released into the supernatant then was assayed by HPLC. HPLC was carried out on a Beckman 125 System Gold, with a model 166 variable-wavelength detector (254 nm used routinely), and data collection was carried out with System Gold software. The separation was on a C18 Ultrasphere column (250 × 4.6 mm; Beckman Instruments) at 1 ml/min using a gradient of CH_3CN in 0.1% TFA to elute CrV. CrV concentrations were determined by comparison of the HPLC peak area to a standard curve. Injecting various known amounts of CrV generated standards.

The concentration of free, supernatant CrV and nonspecifically bound CrV retained in the pellet determined the partition coefficient. This value is the ratio of the nonspecifically bound to free CrV concentrations normalized to the membrane protein concentration in units of mg/ml. The resulting partition coefficient, therefore, has units of $(mg/ml)^{-1}$. The partition coefficient then will predict the fraction of CrV interacting with the membrane if the membrane concentration is known.

Results

Aminotriarylmethane dyes (Fig. 1) share structural similarities with many known NCAs of the AChR. Such similarities include the presence of aromatic groups, tertiary or quaternary amines, and a positive charge. Although this family of basic dyes normally is nonfluorescent, they have high extinction coefficients with absorption maxima in the visible part of the spectrum. To evaluate whether some of the aminotriarylmethane dyes would bind as noncompetitive antagonists of the AChR, we initially screened several of these dyes for their affinity for the NCA site by competitive radioligand-binding assays.

Aminotriarylmethane Dyes Inhibit [^{3}H]Phencyclidine Binding. The ability of several aminotriarylmethane dyes to inhibit [^{3}H]PCP binding to AChR from *Torpedo californica* electric organ was assessed by a centrifugation assay in Torpedo physiological saline (HTPS) using low [^{3}H]PCP concentrations (~1 nM). Preliminary experiments had indicated that addition of the agonist carbamylcholine yielded lower K_{app} values for several of the dyes. Therefore, 100 μM carbamylcholine was routinely included when assaying dyes for binding. Sample curves for five of the dyes are shown in Fig. 2. Each set of data fit well to a curve for inhibition of a single site. The K_{app} values determined from the nonlinear regression (solid lines, Fig. 2) range from 50 nM for crystal violet to 360 μM for Dpmsm, a zwitterionic analog of crystal violet. Table 1 summarizes the measured inhibition constants for all of the compounds tested. Crystal violet, ethyl violet, and methyl violet 2B had K_{app} values of less than 100 nM, values that are substantially lower than those for previously characterized NCAs. New fuchsin, brilliant green, and Victoria blue BO had K_{app} values comparable to those of other high-affinity NCAs in the range of 100 nM to 1 μM. The remaining compounds had K_{app} values in the micromolar range, comparable to many other NCAs. Dpmsm had an exceptionally high K_{app} that likely reflects the presence of a negative charge in the structure.

Examination of CrV and methyl violet 2B by reversed-phase HPLC revealed that commercial methyl violet 2B contained a mixture of compounds: 50% methyl violet, according to the structure in Fig. 1, 40% crystal violet, plus a third peak that was likely the homolog containing only four methyl groups at the amines. Efforts to purify methyl violet from this mixture were unsuccessful. Commercial crystal violet contained small amounts of methyl violet; however, CrV could be purified from the commercial material by crystallization from $CHCl_3$ or from water. The crystallized material that was used for experiments was greater than 95% pure, the only detectable contaminant corresponding to methyl violet. This could not be completely removed, even by repeated crystallization. Because CrV possessed high binding affinity and interesting optical properties, and could be more readily obtained in pure form, it was selected for further characterization. The stoichiometry experiments described below establish that the properties of crystal violet were not due to minor contamination by methyl violet.

Fluorescence and Absorbance Spectra of Crystal Violet. CrV is essentially nonfluorescent in aqueous solution (Fig. 3A) but had been reported to acquire fluorescence upon binding protein (Anderson et al., 1996; Baptista and Indig, 1998). Therefore, we examined the fluorescence of three higher-affinity dyes in the presence of the AChR: CrV, ethyl violet, and new fuchsin. Preliminary experiments indicated that CrV had substantial specific fluorescence enhancement upon binding the AChR. The other two compounds also exhibited fluorescence when added to AChR-rich membranes, but their fluorescence was less susceptible to inhibition by PCP. This suggested less specific fluores-

cence upon binding the NCA site or substantial fluorescence due to nonspecific interactions.

Excitation and emission spectra collected for 10 μM CrV in the absence of AChR confirmed the weak intrinsic fluorescence (Fig. 3A, spectra 3 and 6). In contrast, a 200-fold-lower concentration of 50 nM CrV bound to an excess of AChR (traces 1 and 4) shows 2- to 3-fold-higher fluorescence intensity. Blocking the NCA site with PCP (spectra 2 and 5) can substantially decrease this fluorescence. The residual fluorescence observed in the presence of PCP likely represents fluorescence enhancement of CrV due to nonspecific interaction with the lipid bilayer or with other proteins; the contribution from CrV free in solution was negligible at these concentrations, as indicated by spectra 3 and 6 at a 200-fold higher concentration. Upon binding the AChR, CrV fluorescence increases more than 200-fold with accompanying shifts in the peak excitation and emission wavelengths. The excitation maximum for free CrV shifts from 592 to 599 nm when bound; the emission maximum shifts from 636 nm to 626 nm. Addition of PCP displaces about 75% of the fluorescence signal, indicating that most of the fluorescence enhancement is due to CrV binding to the NCA site of the AChR.

The absorbance spectra of free and AChR-bound CrV (Fig. 3B) show a maximum absorbance at 600 nm for bound CrV (spectrum 2), whereas free CrV (spectrum 1) peaks at 591 nm. The red-shift of 9 nm is consistent with that seen in the corresponding fluorescence excitation spectra (Fig. 3A). Displacement of the bound crystal violet by PCP yields an absorbance maximum similar to AChR-bound CrV (data not shown). At the high membrane concentrations needed to record the absorbance spectrum of bound CrV, a significant fraction of the unbound CrV will interact nonspecifically with the membrane. It is likely that these interactions produce a shift in the absorbance spectrum similar to the shift that occurs upon binding the AChR. The extinction coefficient of CrV does not change substantially upon binding the AChR nor upon interaction with membranes. Therefore, the change in fluorescence intensity represents a change in the quantum yield of the CrV rather than a change in its absorbance properties.

Interaction of Crystal Violet with Membranes. Although the majority of the fluorescence enhancement observed upon CrV binding the AChR was inhibitable by PCP, there was substantial residual fluorescence likely due to nonspecific interactions with the lipid bilayer or with other proteins. Therefore, we used HPLC to quantitate nonspecific interaction with AChR-rich vesicles; this was carried out in

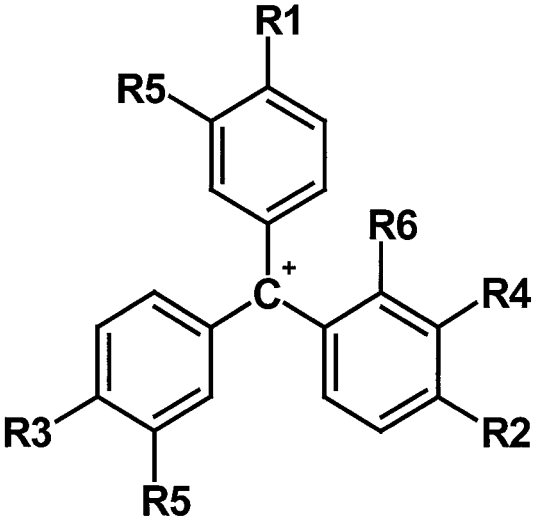

Fig. 1. Structures of aminotriarylmethane dyes. The figure shows the structure of crystal violet and other dyes examined in this study.

Compound	R1	R2	R3	R4	R5	R6
Pararosaniline	NH_2	NH_2	NH_2	H	H	H
Rosaniline	NH_2	NH_2	NH_2	CH_3	H	H
New fuchsin	NH_2	NH_2	NH_2	CH_3	CH_3	H
Malachite green	H	$N(CH_3)_2$	$N(CH_3)_2$	H	H	H
Brilliant green	H	$N(CH_2CH_3)_2$	$N(CH_2CH_3)_2$	H	H	H
Methyl violet	$NHCH_3$	$N(CH_3)_2$	$N(CH_3)_2$	H	H	H
Crystal violet	$N(CH_3)_2$	$N(CH_3)_2$	$N(CH_3)_2$	H	H	H
Ethyl violet	$N(CH_2CH_3)_2$	$N(CH_2CH_3)_2$	$N(CH_2CH_3)_2$	H	H	H
Methyl green	$N^+(CH_3)_2CH_2CH_3$	$N(CH_3)_2$	$N(CH_3)_2$	H	H-	H
Victoria pure blue BO	$N(CH_2CH_3)_2$	$N(CH_3)_2$	$N(CH_2CH_3)_2$	$(CH)_2$-R6	H	$(CH)_2$-R4
Crystal violet lactone	$N(CH_3)_2$	$N(CH_3)_2$	$N(CH_3)_2$	H	H	COO^-
Leuco crystal violet	$N(CH_3)_2$	$N(CH_3)_2$	$N(CH_3)_2$	H	H	H
Dpmsm	$N(CH_3)_2$	OCH_3	$N(CH_3)_2$	SO_3^-	H	H

high concentrations of blocking agents to prevent specific interaction with the high-affinity NCA site on the AChR (see *Experimental Procedures*). We measured the partition coefficient of CrV in both physiological buffer (HTPS, high ionic strength) and at low ionic strength (20 mM HEPES). CrV has a high partition coefficient of 2.62 ± 0.26 $(mg/ml)^{-1}$ ($n = 4$) in physiological buffer. Compare these values with the much lower values determined for ethidium, PCP, and quinacrine (Lurtz et al., 1997) that range from 0.05 to 0.17 $(mg/ml)^{-1}$. In low-ionic-strength buffer, the partition coefficient is 7.48 ± 0.86 $(mg/ml)^{-1}$, ($n = 4$), a value similar to quinacrine, but somewhat higher than ethidium [2 $(mg/ml)^{-1}$] or PCP [0.11 $(mg/ml)^{-1}$]. Thus, under typical conditions used for measuring binding and fluorescence to the AChR (~0.1 mg/ml AChR-rich vesicles), we expect a significant amount (~20%) of nonspecific interaction with the vesicles.

Crystal Violet Binding Measured by Fluorescence Enhancement. The relatively high concentration of AChR (40 nM) limited the ability to measure true K_D values less than this value by inhibition of [^{3}H]PCP binding. This concentration was near the K_{app} values observed for CrV, methyl violet, and perhaps ethyl violet. In these cases, the K_{app} value may reflect titration of the binding sites rather than the true K_D. Therefore, we took advantage of the fluorescence of CrV to measure its K_D for interaction with the AChR by fluorescence enhancement in varying concentrations of CrV (Fig. 4).

Because of its high partition coefficient and its propensity to interact with the surfaces of glass- and plasticware, the free concentration of CrV could not simply be assumed based on the amount of CrV added to the solution. We developed a method to determine directly the solution concentration of CrV using the detergent CHAPS, which also enhances the fluorescence of CrV. After removal of CrV bound to AChR-rich vesicles by centrifugation (see *Experimental Procedures*), the supernatant CrV concentration was readily measured by adding CHAPS to a final concentration of 1% and comparing the fluorescent intensity with a standard curve. This provided a simple means of monitoring free CrV concentrations.

In the presence of excess agonist (Fig. 4A), CrV has a K_D for the AChR of 10 ± 3 nM; in the absence of agonist the affinity is near 100 ± 50 nM (Fig. 4B; summarized in Table 2). In each case, the data were fit to the binding isotherm (eq. 2). The data saturate and are consistent with the presence of a single binding site. The determination of the K_D in the absence of agonist was substantially more variable. This was due to the higher nonspecific fluorescence encountered at the higher CrV concentrations needed to approach saturable binding. Similar experiments conducted for CrV in low-ionic-strength buffer indicate K_D values of less than 1 nM (data not shown); however, accurate dissociation constants were not obtained because the CHAPS method for determining free CrV concentrations could not accurately measure CrV below 1 nM. Nonetheless, the ionic strength effects on the CrV K_D are consistent with a substantial charge dependence of binding, as was observed for ethidium, PCP, quinacrine, and

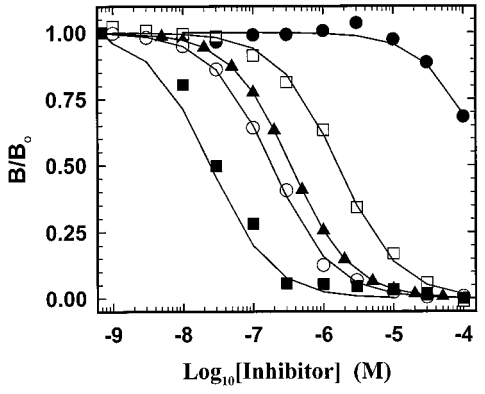

Fig. 2. Inhibition of [^{3}H]phencyclidine binding by aminotriarylmethane dyes. AChR-rich membranes (100 μg; 40 nM AChR, 1 ml volume) were incubated in HTPS buffer at ambient temperature (20°C) with 1 nM [^{3}H]PCP in the presence of 100 μM carbamylcholine and the indicated concentrations of dye. Bound [^{3}H]PCP was determined as described under *Experimental Procedures*. Data from each curve were fit to eq. 1 (solid lines), and K_{app} values were determined for each: Dpmsm, 360 μM (●), pararosaniline, 1.6 μM (□), brilliant green, 340 nM (▲), new fuchsin, 190 nM (○), and crystal violet, 28 nM (■). Each symbol represents the average of duplicate determinations. Data from separate experiments were normalized to the maximum [^{3}H]PCP bound and combined in a single figure.

TABLE 1

K_{app} for aminotriarylmethane dyes

K_{app} values were determined by inhibition of [^{3}H]PCP binding as described in *Experimental Procedures* and in Fig. 2. The errors are the S.D.s from n independent determinations.

Compound	K_{app}	n
	μM	
Pararosaniline	2.2 ± 0.97	3
Rosaniline	1.3 ± 0.87	4
New fuchsin	0.4 ± 0.15	4
Malachite green	3.9 ± 2.64	3
Brilliant green	0.3 ± 0.07	3
Methyl violet 2B	0.07 ± 0.03	3
Crystal violet	0.05 ± 0.03	6
Ethyl violet	0.08 ± 0.02	4
Methyl green	7.2 ± 0.3	2
Victoria pure blue BO	0.13 ± 0.11	3
Dpmsm	360.0 ± 190	3

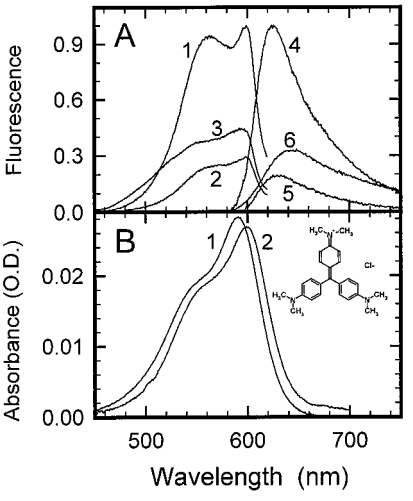

Fig. 3. Fluorescence and absorbance spectra of crystal violet. A, excitation spectra (traces 1 and 2) and emission spectra (traces 4 and 5) for 50 nM crystal violet incubated in HTPS with 100 nM AChR and 1 mM carbamylcholine were collected as described in *Experimental Procedures*. Spectra were taken in the absence (spectra 1 and 4) or presence of 100 μM PCP (spectra 2 and 5). Excitation and emission spectra of 10 μM crystal violet in HTPS without AChR present are shown for comparison (spectra 3 and 6, respectively). Each set of excitation and emission spectra was normalized to the peak value for CrV bound to the AChR. B, absorbance spectra of 400 nM crystal violet in HTPS (spectrum 1) or bound to AChR-rich vesicles (512 nM AChR, spectrum 2). The inset shows the structure of crystal violet chloride. The peak wavelengths for the spectra are as follows: A, spectra 1, 599 nm; 2, 599 nm; 3, 593 nm; 4, 626 nm; 5, 633 nm; 6, 640 nm. B, spectra 1, 591 nm; 2, 600 nm.

meproadifen (Lurtz et al., 1997), and with competition for channel-permeant ions.

Crystal Violet Interaction with the Agonist-Binding Sites. The approximately 10-fold decrease in the K_D value for CrV in the presence of agonist suggested that a reciprocal effect of CrV on agonist binding should exist. We examined the affinity of [^{3}H]ACh in varying concentrations of CrV (Fig. 5). Using low concentrations of AChR and low concentrations of high specific radioactivity [^{3}H]ACh, we measured the ratio of bound to free [^{3}H]ACh at increasing concentrations of CrV or proadifen (Fig. 5). At conditions in which only a small percentage of the sites are bound with ligand, the bound-to-free ratio of [^{3}H]ACh is proportional to the affinity of [^{3}H]ACh (i.e., inversely proportional to the K_D). The bound-to-free ratio increases nearly 10-fold in the presence of either added ligand, consistent with an increase in [^{3}H]ACh affinity to the AChR. The CrV curve is to the left of the proadifen curve, indicating that CrV was more potent, consistent with its higher affinity. The decrease in the bound-to-free ratio of [^{3}H]ACh observed at the higher concentrations of NCA likely reflects direct competition for binding at the agonist sites. CrV appears to interact with the ACh sites with an IC_{50} of 30 μM and with proadifen with an IC_{50} of ~300 μM.

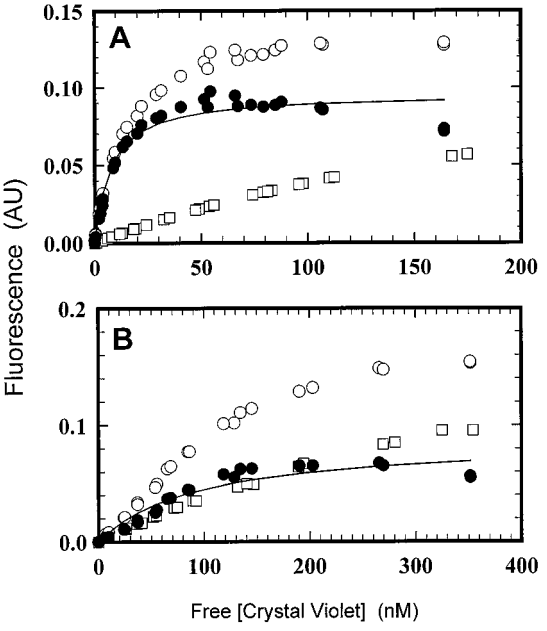

Fig. 4. Equilibrium-binding crystal violet as measured by fluorescence intensity. AChR-rich membranes (20 nM AChR, 1.5 ml) were incubated in HTPS at ambient temperature with varying concentrations of crystal violet in the absence (○) or presence (□) of 0.1 mM PCP. The experiments were either in the presence (A) or in the absence (B) of 100 μM carbamylcholine. The fluorescence intensity was measured for each sample as described in *Experimental Procedures*. After removal of bound crystal violet by centrifugation, free crystal violet was quantified by fluorescence in CHAPS and as described in *Experimental Procedures*. Specific binding (●) was determined after subtraction of nonspecific binding from the fluorescence intensity measured in the absence of PCP. The solid lines represent the best fits to the binding equation (eq. 2). As determined by the fitting, the K_D was 7.6 nM and the maximal specific fluorescence was 0.096 (A), and the K_D was 93 nM and the maximal specific fluorescence was 0.087 (B).

TABLE 2

Comparison of K_{app} and IC_{50} values for crystal violet interaction with the AChR in the presence and absence of agonist

K_{app} and IC_{50} values were determined by the various methods as described in *Experimental Procedures* and the individual figure legends. The averages and S.D.s are shown with the number of individual experiments in parentheses. N.D. indicates the measurement was not done.

Method	K_{app}	
	− Carb	+ Carb
	nM	
Fluorescence	100 ± 46 (5)	10 ± 3.4 (2)
[^{3}H]Phencyclidine	1200 ± 140 (2)	50 ± 30 (6)
[^{3}H]Acetylcholine	860 ± 120 (3)	N.D.
^{22}Na flux	1700 ± 840 (4)	N.D.

Crystal Violet Binds Competitively with the PCP. Fluorescence binding data (Fig. 4) and [^{3}H]PCP inhibition data (Fig. 2) were consistent with CrV binding to the high-affinity noncompetitive antagonist site of the AChR. On this basis alone, however, an allosteric mechanism of inhibition could not be ruled out altogether. Other NCAs have multiple sites of binding associated with the AChR (Heidmann et al., 1983) and may be able to influence the conformation of the AChR through nonspecific interactions (Boyd and Cohen, 1984). We therefore examined the PCP inhibition of CrV binding at several CrV concentrations, using CrV fluorescence as an indicator of binding. For each curve, the CrV concentration was held constant and the fluorescence was measured in the presence of increasing PCP concentrations (Fig. 6).

Each set of data was fit to the model for single site inhibition, and the K_{app} values for PCP were derived. The K_{app} values for PCP were replotted as a function of CrV concentration (Fig. 6, inset). For a competitive mechanism of binding the replot is expected to be linear where $K_{app} = K_{PCP} + [CrV](K_{PCP}/K_{CrV})$. The corresponding plot for an allosteric mechanism of inhibition has a hyperbolic form that will saturate at high CrV concentrations (Wang et al., 1996). For the competitive mechanism the slope of the line is the ratio of the K_D values for PCP and for CrV; the measured linear slope from the replot in Fig. 6 is 15, a value that corresponds well to the value of 30 obtained from the ratio of K_D values of PCP (~300 nM; Lurtz et al., 1997) and CrV (10 nM, Table 2). The linear replot of the K_{app} values is consistent with inhibition by PCP by binding at the same locus. Although the data cannot *absolutely* exclude an allosteric mechanism, the high concentrations of CrV used (2- to 40-fold higher than its K_D)

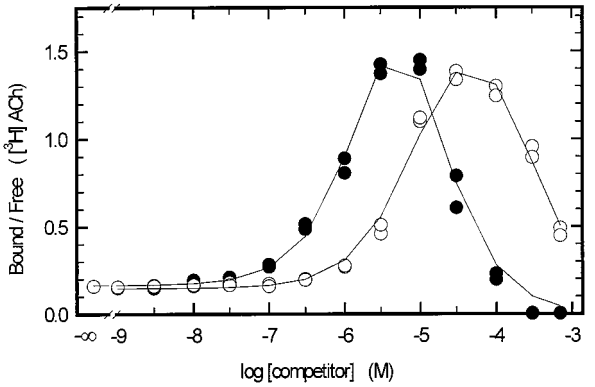

Fig. 5. Crystal violet increases [^{3}H]ACh affinity. AChR-rich membranes (12 nM AChR) were incubated in HTPS in the presence of ~1 nM [^{3}H]ACh and in the presence of increasing concentrations of either proadifen (○) or CrV (●). Bound and free concentrations of [^{3}H]ACh were determined as described in *Experimental Procedures*. Data were plotted as bound divided by free [^{3}H]ACh. Each curve illustrates the increase in [^{3}H]ACh binding due to an increased affinity for the AChR in the presence of desensitizing ligand.

would require extremely strong interactions between two independent sites such that binding to one causes greater than 40-fold changes in the affinity of the second ligand. This result, therefore, strongly suggests that CrV fluorescence enhancement occurs by binding the same site as PCP on the AChR.

Stoichiometry of Crystal Violet Binding to the AChR. Binding data from both radioligand inhibition assays and direct binding experiments are consistent with CrV binding to a single class of sites on the AChR. To quantitate the number of CrV-binding sites on the AChR associated with the fluorescence enhancement, CrV was titrated into a concentrated suspension of AChR-rich vesicles and the fluorescence was measured (Fig. 7). At low concentrations, nearly all of the CrV added bound to the AChR and the fluorescence increased linearly; the slope of this line reflects the fluorescence yield (per nM CrV) due to binding the AChR. At higher concentrations of CrV, the binding sites become saturated, and the fluorescence signal increased linearly with a lower slope. A similar slope was observed at the higher CrV concentrations titrated into AChR-rich vesicles in the presence of PCP to block binding to the NCA site. The limiting slope at the higher CrV concentrations, therefore, reflects the fluorescence increase due to nonspecific interactions. At the intersection of these lines, the added CrV concentration equals the total binding-site concentration (see *Experimental Procedures*). This value can be compared with the AChR concentration added based on [^{3}H]ACh binding, which routinely is used to quantitate various AChR-rich vesicle preparations. The ratio is 1.06 ± 0.17 CrV binding sites per AChR for four independent determinations carried out as shown in Fig. 7. This value suggests that CrV binds a single high-affinity site on the AChR, which is consistent with binding to the central ion pore.

Crystal Violet Blocks ^{22}Na Efflux from AChR-Rich Vesicles. To determine the effect of CrV on AChR function, we examined the ability of CrV to block ^{22}Na efflux from AChR-rich vesicles. Efflux was elicited by the addition of the partial agonist phenyltrimethylammonium (PTMA). Preliminary experiments established that 0.3 mM PTMA yielded maximum agonist-stimulated efflux, a level of efflux that was usually 60 to 70% of that released by the ionophore gramicidin. Preincubation of AChR-rich vesicles with a CrV concentration of 1 to 10 μM blocked agonist-stimulated efflux with an average IC_{50} of 1.7 ± 0.8 μM (Fig. 8; Table 2). This value can be compared to the average IC_{50} of 19 ± 6 μM for PCP. This IC_{50} was consistent with that observed previously by others (White et al., 1991).

At higher concentrations, there is apparent loss of the block of efflux by CrV. Control experiments established that the ^{22}Na efflux observed at high levels was independent of the addition of agonist and could not be blocked by the antagonist *d*-tubocurarine. At these concentrations, CrV appears to cause ^{22}Na efflux from the vesicles independent of its interaction with the AChR. This observation is consistent with the strong ability of CrV to interact with the membrane as measured by its partition coefficient.

Discussion

We have shown that various basic aminotriarylmethane dyes bind to the NCA site of the AChR. By characterizing one of these dyes, CrV, in detail we have shown that it possesses the characteristics of many high-affinity noncompetitive antagonists that bind the M2 region of the AChR and block activity by steric hindrance of ion passage through the pore of the AChR. These characteristics include high-affinity binding (~10 nM) for a single site on the AChR, higher affinity in the presence of agonist than for the resting conformation, competitive binding with PCP, the ability to allosterically interact with the agonist-binding sites, and the ability to block ^{22}Na efflux from AChR-rich vesicles. The K_{app} values for these properties are summarized in Table 2. There is good agreement between the potencies of CrV to inhibit ^{22}Na efflux, enhance [^{3}H]ACh affinity, and block [^{3}H]PCP binding in the absence of agonist (data not shown), all at concentrations near 1 μM. The primary difference is between those values and the directly measured K_D in the absence of agonist (100 nM, Table 2). The reason for this difference is not entirely clear, but may reflect difficulty in obtaining precise data for the K_D by fluorescence enhancement because of the

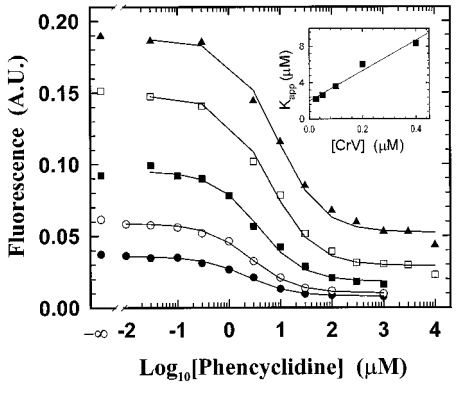

Fig. 6. Inhibition of crystal violet fluorescence by phencyclidine. AChR-rich membranes (20 nM) were incubated in HTPS in the presence of 0.1 mM carbamylcholine, with 25 nM (●), 50 nM (○), 100 nM (■), 200 nM (□), or 400 nM (▲) crystal violet and increasing concentrations of PCP. The fluorescence intensity at each PCP concentration for each crystal violet concentration is plotted. Symbols represent the average of duplicate determinations. Each curve was fit to a binding isotherm for a single site inhibition. K_{app} values for PCP were replotted as a function of CrV concentration (inset). The slope of the replot was determined by linear regression.

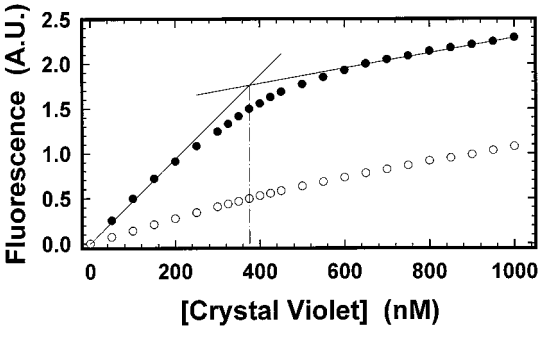

Fig. 7. Stoichiometry of crystal violet binding to the AChR. AChR-rich membranes (375 nM AChR) were incubated in the presence of 0.1 mM carbamylcholine in HTPS (●). CrV was titrated into the membranes, and the fluorescence intensity was monitored. The titration was repeated in the presence of 1 mM PCP (○) to define nonspecific fluorescence. Linear regressions were applied to initial and ending linear components of the titration in the absence of PCP (0–200 nM CrV and 650–1000 nM CrV, respectively). The intercept from these two sets of points is 376 nM and defines the concentration of CrV-binding sites (see *Experimental Procedures*).

higher nonspecific binding at the CrV concentrations required to measure binding in the absence of agonist.

The discrepancy between the K_{app} measured by fluorescence enhancement and by [^{3}H]PCP binding in the presence of agonist (Table 2) simply reflects the lower limit of the [^{3}H]PCP-binding assay; the value determined by fluorescence likely reflects the true K_D. Comparison of the K_{app} values in the absence of agonist versus those in the presence of agonist suggests that CrV binding strongly favors the desensitized conformation of the AChR because this is the conformation stabilized by agonists at equilibrium. Nonetheless, CrV potentially could be acting as an open channel blocker or trapping the AChR in a distinct conformation with high affinity for agonist. These possibilities may be resolved by examination of the kinetics of binding using either fluorescence methods or by single channel measurements of blockade. The preferential binding in the presence of agonist is consistent with the observation that larger NCAs preferentially bind the desensitized state of the AChR, whereas ligands that prefer binding to the resting conformation, such as tetracaine or TID, tend to be smaller (Cohen et al., 1986; White and Cohen, 1992). This trend also favors the model of Furois-Corbin and Pullman and of White and Cohen that suggests that the pore of the AChR expands at the synaptic end upon desensitization by tilting of the M2 α-helices away from the central axis of the AChR (Furois-Corbin and Pullman, 1989; White and Cohen, 1992).

Several of the other dyes bind with affinities comparable to CrV, and many of the dyes display similar properties, including higher affinity for the desensitized state as measured by inhibition of [^{3}H]PCP binding (brilliant green, malachite green, rosaniline, ethyl violet; data not shown). Therefore, the affinities of the various dyes can be compared in terms of binding a single site on the AChR. The detailed structure-activity relationship of these dyes will be particularly interesting as they represent a large class of compounds with well developed chemistry. This will permit a closer examination of the structure of the pore of the AChR than has been possible with the previously known heterogeneous collection of ligands.

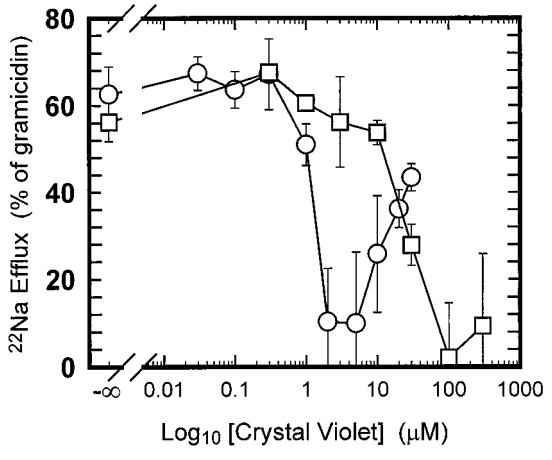

Fig. 8. Crystal violet inhibits ^{22}Na efflux from *Torpedo californica* vesicles. AChR-rich vesicles (90 nM AChR) that had been loaded with ^{22}Na were incubated in HTPS (1 ml) in the presence of varying concentrations of CrV (○) or PCP (□) for 10 min on ice. ^{22}Na efflux was initiated by the addition of PTMA (0.3 mM final concentration). After 20 s, samples were immediately filtered and washed with 10 ml ice-cold HTPS as described in *Experimental Procedures*. Data are plotted as the percentage of counts released relative to the release induced by gramicidin. Gramicidin-releasable counts typically ranged from 400 to 800 cpm with a filter background of 200 to 400 cpm. The IC_{50} for inhibition of efflux by CrV was 1.3 μM and by PCP was 25 μM. Each symbol and error bar represent the average and S.D. of three determinations.

Structure Activity Relationship of the Basic Dyes. The dyes examined have several discrete, small changes in structure that cause significant changes in affinity (see Fig. 1 for reference). The six methyls on the CrV-amines contribute substantially to affinity. Pararosaniline has none of these methyls and binds with ~200-fold lower affinity (compare K_{app} = 2200 nM for pararosaniline, Table 1, with K_D = 10 nM for CrV, Table 2). Removal of one complete dimethylamino group also substantially lowers affinity (compare malachite green, K_{app} = 3.9 μM, with CrV, K_D = 10 nM). Increasing the size of the amine substituents from methyl to ethyl groups improves affinity: compare the K_{app} values of malachite green and brilliant green. Likewise, ethyl violet has a K_{app} similar to CrV, but because the K_{app} estimate was limited by the AChR concentration, a precise comparison will require further experiments.

Substitutions at the positions ortho and meta to the central carbon also increase affinity. Comparison of pararosaniline, rosaniline, and new fuchsin shows enhanced affinity with methylation at the positions meta to the central carbon. As a caveat, however, it should be noted that rosaniline contained at least 14 separable components when examined by HPLC (data not shown). The compound Victoria blue BO includes an additional fused aromatic ring. The added bulk appears to inhibit binding only moderately as it binds with a K_{app} slightly higher than its congeners, ethyl violet and CrV. The increased bulk and hydrophobicity in this region does not, therefore, substantially interfere with binding and, in the case of the pararosaniline series, enhances binding.

CrV bears a single, delocalized positive charge. The zwitterionic analog, Dpmsm, binds with very low affinity (K_D > 300 μM). This compound has one of the dimethylamino groups replaced by a methoxy group and a sulfate moiety in a position meta to the central carbon (Fig. 1). Although the methoxy may contribute to some of the affinity loss, a significant amount likely is due to the presence of the negative charge added. In contrast, methyl green is dicationic with an additional *N*-ethyl group and binds 700-fold more weakly (K_{app} ~ 7000 nM, Table 1) than CrV. It appears that addition of either the ethyl group or the second charge alters the interaction substantially.

However, as argued above, increased steric bulk on the amines does not dramatically decrease affinity. Therefore, it seems unlikely that the steric bulk of the added ethyl group on methyl green, as compared with CrV, would substantially affect binding. A similar observation was made for analogs of *d*-tubocurarine: addition of a single methyl group at the 2′-nitrogen of tubocurine (converting it to *d*-tubocurarine) decreased the affinity for the NCA site ~100-fold (Pedersen and Papineni, 1995). This addition, however, did not alter the net charge of +2 on the curare compound. The distances between the two charged nitrogens on *d*-tubocurarine (10.5 Å) is similar to the distance between two dimethylamines on CrV (9.8 Å) and the distance between the two arylamines of ethidium (9.8 Å). These observations suggest the importance of nonquaternary amines in a particular arrangement, perhaps to act as hydrogen bond acceptors or participate in other specific interactions with the pore of the channel.

Fluorescence of Crystal Violet. The fluorescence enhancement that accompanies binding of CrV to the AChR is greater than 200-fold and is due to a change in quantum yield, as shown by the small changes in the absorbance spectrum (Fig. 3). This large enhancement is possible because CrV is only weakly fluorescent in aqueous solution. The weak fluorescence is attributed to rapid de-excitation of the excited state by concerted rotation of the three aryl rings (Duxbury, 1993). Binding to the AChR likely inhibits this rotation, eliminating this mechanism of de-excitation, and results in a much higher quantum yield. The Stokes shift, the difference between the peak emission and absorbance wavelengths, decreased substantially upon AChR binding, indicative of binding in a nonpolar environment (Lakowicz, 1983). This conclusion is consistent with the generally nonpolar nature of the residues associated with the M2 sequences of the AChR that comprise the high-affinity NCA-binding site.

In addition to structure-activity analysis, the dyes we have examined are likely to have substantial utility in future experiments to characterize the AChR pore. The high-affinity dyes (new fuchsin, brilliant green, crystal violet, and ethyl violet) have large molar extinction coefficients across a broad portion of the visible spectrum. They can serve as excellent fluorescence energy transfer acceptors from a variety of donors. The properties of CrV make it suitable for fluorescence quenching studies to examine the environment of the pore of the AChR, whereas other fluorescent ligands such as ethidium and quinacrine have been limited by their moderate affinity. Another intriguing possibility is to use this ligand as a source of heat or free radicals for site-directed protein modification. Malachite green has been shown to cause local heating that results in protein damage (Indig et al., 1992). Preliminary experiments show that CrV indeed sensitizes the AChR to free radical damage in the presence of light (W. H. Vila-Carriles and S.E.P., unpublished observations).

One drawback to using CrV is its substantial nonspecific interactions with the membrane, with plastic surfaces, and with glass. This creates difficulties in quantitation of CrV itself. However, most of these problems can be overcome by explicit measurements of CrV concentration by the CHAPS assay or by HPLC. Treatment of glass with polyethyleneimine or cationic silanes also prevents CrV from sticking to glassware and permits it to be transferred reproducibly and without loss. The high affinity of CrV largely compensates for this inconvenience of nonspecific binding artifacts.

Acknowledgments

We thank Arlene Samano for excellent technical assistance in carrying out many ligand-binding assays.

References

Anderson GB, de Arruda MV and Indig GL (1996) Binding of triarylmethane dyes to proteins: Enhanced fluorescence quantum yield and photoreactivity. *Biophys J* **70:**A211.

Baptista MS and Indig GL (1998) Effect of BSA binding on photophysical and photochemical properties of triarylmethane dyes. *J Phys Chem B* **102:**4678–4688.

Boyd ND and Cohen JB (1984) Desensitization of membrane-bound *Torpedo* acetylcholine receptor by amine noncompetitive antagonists and aliphatic alcohols: Studies of [^{3}H]acetylcholine binding and $^{22}Na^+$ ion fluxes. *Biochemistry* **23:**4023–4033.

Charnet P, Labarca C, Leonard RJ, Vogelaar NJ, Czyzyk L, Gouin A, Davidson N and Lester HA (1990) An open-channel blocker interacts with adjacent turns of alpha-helices in the nicotinic acetylcholine receptor. *Neuron* **4:**87–95.

Cohen JB, Correll LA, Dreyer EB, Kuisk IR, Medynski DC and Strnad NP (1986) Interactions of Local Anesthetics with Torpedo Nicotinic Acetylcholine Receptors, in *Molecular and Cellular Mechanisms of Anesthetics* (Roth SH and Miller KW eds) pp 111–124, Plenum, New York.

Duxbury DF (1993) The photochemistry and photophysics of triphenylmethane dyes in solid and liquid media. *Chem Rev* **93:**381–433.

Furois-Corbin S and Pullman A (1989) A possible model for the inner wall of the acetylcholine receptor channel. *Biochim Biophys Acta* **984:**339–350.

Giraudat J, Dennis M, Heidmann T, Chang JY and Changeux JP (1986) Structure of the high-affinity binding site for noncompetitive blockers of the acetylcholine receptor: Serine-262 of the delta subunit is labeled by [^{3}H]chlorpromazine. *Proc Natl Acad Sci USA* **83:**2719–2723.

Giraudat J, Dennis M, Heidmann T, Haumont PY, Lederer F and Changeux JP (1987) Structure of the high-affinity binding site for noncompetitive blockers of the acetylcholine receptor: [^{3}H]Chlorpromazine labels homologous residues in the beta and delta chains. *Biochemistry* **26:**2410–2418.

Giraudat J, Gali J, Revah F, Changeux J, Haumont P and Lederer F (1989) The noncompetitive blocker [^{3}H]chlorpromazine labels segment M2 but not segment M1 of the nicotinic acetylcholine receptor alpha-subunit. *FEBS Lett* **253:**190–198.

Heidmann T, Oswald RE and Changeux JP (1983) Multiple sites of action for noncompetitive blockers on acetylcholine receptor rich membrane fragments from torpedo marmorata. *Biochemistry* **22:**3112–3127.

Herz JM and Atherton SJ (1992) Steric factors limit access to the noncompetitive inhibitor site of the nicotinic acetylcholine receptor: Fluorescence studies. *Biophys J* **62:**74–76.

Herz JM, Johnson DA and Taylor P (1987) Interaction of noncompetitive inhibitors with the acetylcholine receptor: The site specificity and spectroscopic properties of ethidium binding. *J Biol Chem* **262:**7238–7247.

Hucho F, Oberthur W and Lottspeich F (1986) The ion channel of the nicotinic acetylcholine receptor is formed by the homologous helices M II of the receptor subunits. *FEBS Lett* **205:**137–142.

Imoto K, Busch C, Sakmann B, Mishina M, Konno T, Nakai J, Bujo H, Mori Y, Fukuda K and Numa S (1988) Rings of negatively charged amino acids determine the acetylcholine receptor channel conductance. *Nature (London)* **335:**645–648.

Imoto K, Methfessel C, Sakmann B, Mishina M, Mori Y, Konno T, Fukuda K, Kurasaki M, Bujo H, Fujita Y and Numa S (1986) Location of a delta-subunit region determining ion transport through the acetylcholine receptor channel. *Nature* **324:**670–674.

Indig GL, Jay DG and Grabowski JJ (1992) The efficiency of malachite green, free and protein bound, as a photon-to-heat converter. *Biophys J* **61:**631–638.

Krodel EK, Beckman RA and Cohen JB (1979) Identification of a local anesthetic binding site in nicotinic post-synaptic membranes isolated from *Torpedo marmorata* electric tissue. *Mol Pharmacol* **15:**294–312.

Lakowicz (1983) *Principles of Fluorescence Spectroscopy*, Plenum, New York.

Leonard RJ, Labarca CG, Charnet P, Davidson N and Lester HA (1988) Evidence that the M2 membrane-spanning region lines the ion channel pore of the nicotinic receptor. *Science* **242:**1578–1581.

Lurtz MM, Hareland ML and Pedersen SE (1997) Quinacrine and ethidium bromide bind the same locus on the nicotinic acetylcholine receptor from *Torpedo californica*. *Biochemistry* **36:**2068–2075.

Neher E and Steinbach JH (1978) Local anaesthetics transiently block currents through single acetylcholine-receptor channels. *J Physiol (London)* **277:**153–176.

Neubig RR and Cohen JB (1980) Permeability control by cholinergic receptors in *Torpedo* postsynaptic membranes: Agonist dose-response relations measured at second and millisecond times. *Biochemistry* **19:**2770–2779.

Noda M, Takahashi H, Tanabe T, Toyosato M, Kikyotani S, Furutani Y, Hirose T, Takashima H, Inayama S, Miyata T and Numa S (1983) Structural homology of *Torpedo californica* acetylcholine receptor subunits. *Nature (London)* **302:**528–532.

Pedersen SE, Dreyer EB and Cohen JB (1986) Location of ligand-binding sites on the nicotinic acetylcholine receptor alpha-subunit. *J Biol Chem* **261:**13735–13743.

Pedersen SE and Papineni RV (1995) Interaction of *d*-tubocurarine analogs with the *Torpedo* nicotinic acetylcholine receptor: Methylation and stereoisomerization affect site-selective competitive binding and binding to the noncompetitive site. *J Biol Chem* **270:**31141–31150.

Pedersen SE, Sharp SD, Liu WS and Cohen JB (1992) Structure of the noncompetitive antagonist-binding site of the *Torpedo* nicotinic acetylcholine receptor. *J Biol Chem* **267:**10489–10499.

Raftery MA, Hunkapiller MW, Strader CD and Hood LE (1980) Acetylcholine receptor: Complex of homologous subunits. *Science* **208:**1454–1456.

Sobel A, Weber M and Changeux J-P (1977) Large-scale purification of the acetylcholine-receptor protein in its membrane-bound and detergent extracted forms from *Torpedo marmorata* electric organ. *Eur J Biochem* **80:**215–224.

Stryer L, Thomas DD and Meares CF (1982) Diffusion-enhanced fluorescence energy transfer. *Annu Rev Biophys Bioeng* **11:**203–222.

Unwin N (1993) Nicotinic acetylcholine receptor at 9 Å resolution. *J Mol Biol* **229:**1101–1124.

Wang JP, Needleman DH, Seryshev AB, Aghdasi B, Slavik KJ, Liu SQ, Pedersen SE and Hamilton SL (1996) Interaction between ryanodine and neomycin binding sites on Ca^{2+} release channel from skeletal muscle sarcoplasmic reticulum. *J Biol Chem* **271:**8387–8393.

White BH and Cohen JB (1992) Agonist-induced changes in the structure of the acetylcholine receptor M2 regions revealed by photoincorporation of an uncharged nicotinic noncompetitive antagonist. *J Biol Chem* **267:**15770–15783.

White BH, Howard S, Cohen SG and Cohen JB (1991) The hydrophobic photoreagent 3-(trifluoromethyl)-3-m-([^{125}I]iodophenyl) diazirine is a novel noncompetitive antagonist of the nicotinic acetylcholine receptor. *J Biol Chem* **266:**21595–21607.

Wu G, Raines DE and Miller KW (1994) A hydrophobic inhibitor of the nicotinic acetylcholine receptor acts on the resting state. *Biochemistry* **33:**15375–15381.

Send reprint requests to: Dr. Steen E. Pedersen, Department of Molecular Physiology and Biophysics, Baylor College of Medicine, One Baylor Plaza, Houston, TX 77030. E-mail:pedersen@bcm.tmc.edu